Supporting Information

Hydrophilic Monodisperse Magnetic Nanoparticles Protected by an Amphiphilic Alternating Copolymer

Eleonora V. Shtykova, Xinlei Huang, Xinfeng Gao, Jason C. Dyke, Abrin L. Schmucker, Nicholas Remmes, David V. Baxter, Barry Stein, Bogdan Dragnea, Peter V. Konarev, Dmitri I. Svergun, Lyudmila M. Bronstein**

1. TEM and XRD

The TEM images of the NPs are presented in Figure S1. Spherical monodisperse NPs of 16.1 nm in diameter and a standard deviation of 3.7% (**NP1)** (Fig. S1a) and 20.5 nm in diameter and a standard deviation of 4.1 % (**NP2)** (Fig. S1b) were prepared from the iron oleate precursor FeOl4,[1] where oleic acid (which is a byproduct of the synthesis via sodium oleate) was removed by extraction (see Experimental part). The iron oleate precursor FeOl2,[1] which was not undergone extraction and included oleic acid in its structure, gave NPs with a diameter of 20.8 nm and a standard deviation of 4.0% (**NP3)** (Fig. S1c). The presence or absence of oleic acid in the iron oleate structure also results in different coordination of an oleate ligand as discussed in our earlier paper.[1] In FeOl2 one Fe(III) is connected to one bidentate and one unidentate oleates, while FeOl4 is more densely packed with only one bidentate oleate per each Fe(III).

Independently of the type of iron oleate used, similar sizes can be obtained in the same solvent (compare images in Fig. S1, b and c). It is noteworthy, though, that in the syntheses with FeOl4 higher

* To whom correspondence should be addressed (lybronst@indiana.edu, svergun@embl-hamburg.de)

loading of oleic acid should be used to stabilize NPs as FeOl4 does not contain oleic acid impurities while FeOl2 does (see also ref.[1]). The variation of the oleic acid loading can allow some variation of the particle size: a ~7% increase of the oleic acid loading (1.6 mL vs 1.5 mL) leads to a 20% decrease of the NP diameter (16.1 nm vs 20.5 nm) (Fig. S1, a and b). Despite the different iron oleate precursors, the XRD patterns of **NP2** and **NP3** are similar showing both wüstite ($Fe_{(1-x)}O$) and spinel (most likely Fe_3O_4) phases (Fig. 2). The wüstite crystals are larger (the signals are more narrow) than the spinel crystals (the signals are broader) (see also ref.[1]).

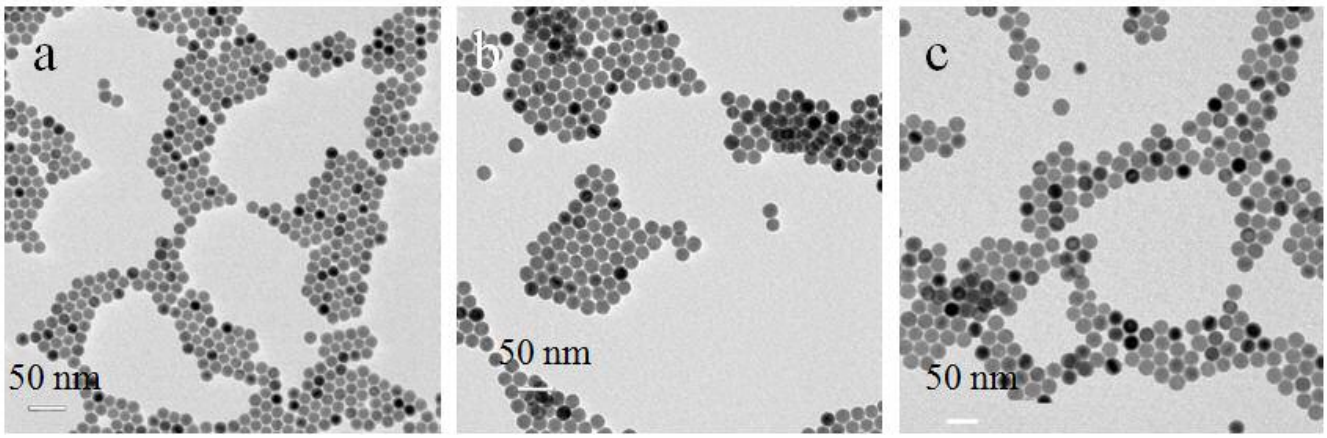

Figure S1. TEM images of **NP1** (a), **NP2** (b), and **NP3** (c).

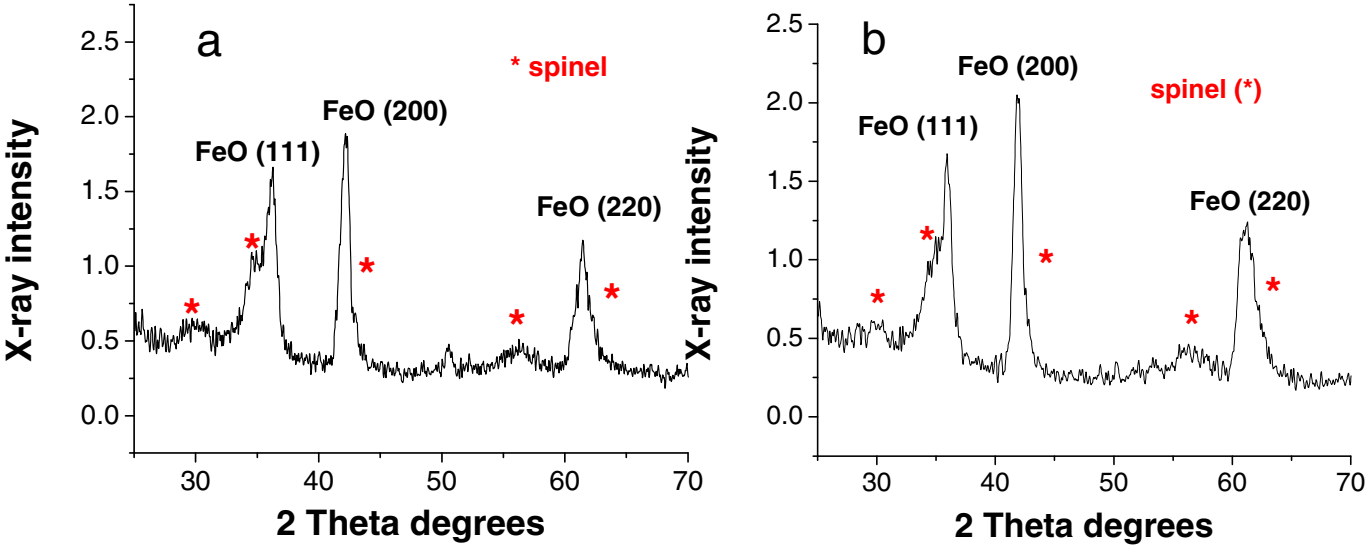

Figure S2. XRD profiles of **NP2** (a) and **NP3** (b).

2. Magnetic measurements

Magnetic measurements were carried out for the **NP1** and **NP2** samples (magnetic measurements for **NP3** are described in our preceding papers[2, 3]). The ZFC/FC curves on each sample are shown in Figure 3. In the region where the ZFC and FC curves overlap the sample is assumed to be superparamagnetic. The average blocking temperatures (T_b) of the **NP1** and **NP2** samples are about 220 K and 200 K, respectively (Fig. 3). The lower T_b value for **NP1** than for **NP2** is consistent with the difference in the NP size. It should be noted that the blocking temperature of **NP3** is ~250 K,[2] suggesting that despite sizes and XRD profiles of **NP2** and **NP3** are similar, the structural organization of these NPs (and anisotropy), influencing their magnetic properties, should be different.

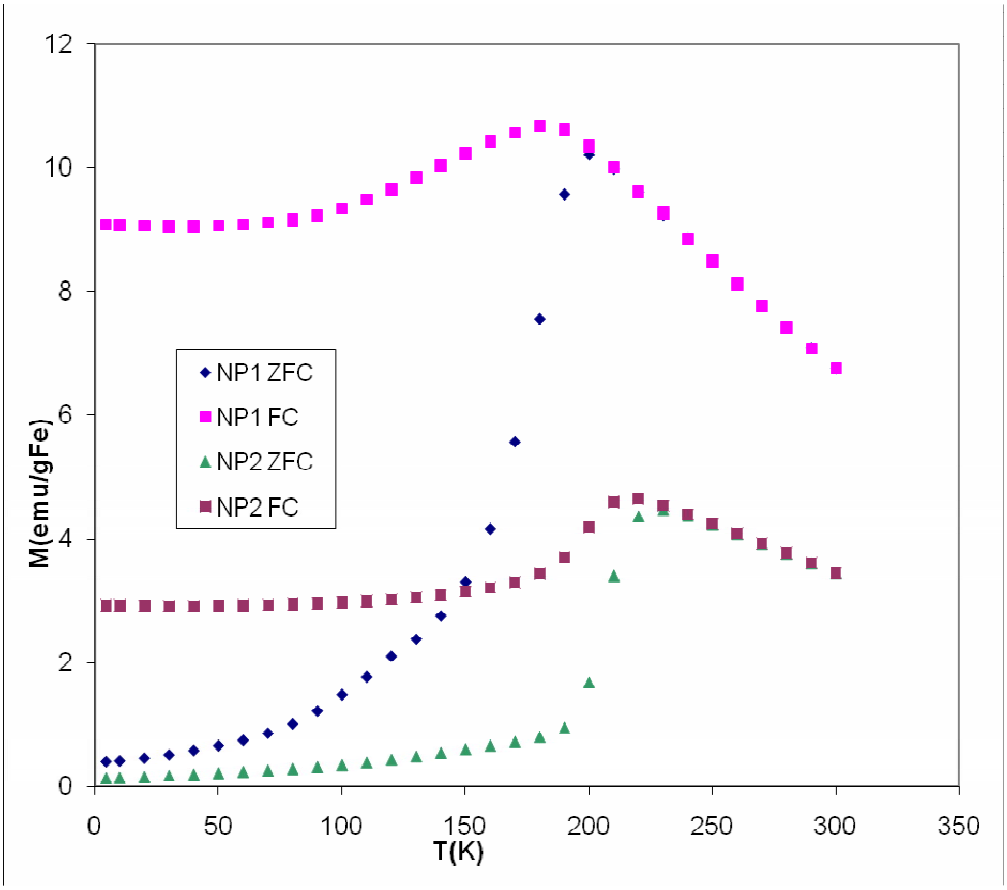

Figure S3. ZFC/FC for **NP1** and **NP2** at 50 Oe (top)

3. FTIR

As-prepared **NP1** and **NP3** were characterized by FTIR (Fig. S5). (It is noteworthy that the FTIR spectra of **NP1** and **NP2** are similar, so the latter are not shown.) Comparison of the intensity ratio of the bands at 2917 and 2848 cm^1 characteristic of CH_2 groups of oleic acid[5] and the band at about 573 cm^{-1} characteristic of Fe-O moieties[6, 7] allows rough estimation of the amount of stabilizing molecules on the NP surface. This comparison shows that the **NP1** shell contains a higher amount of oleic acid ligands. Moreover, in the FTIR spectrum of **NP1** there is the band at 1711 cm^{-1}, which is typical of the COOH groups.[5] This suggests the presence of non-adsorbed or weakly adsorbed oleic acid, which is absent in the **NP3** sample. Because the **NP1** and **NP3** samples were similarly purified (see Experimental part), the excess of oleic acid which is not included in a hydrophobic shell was removed. Thus non-adsorbed oleic acid is retained in the **NP1** shell. Scheme S1 depicts most probable shell structure of the **NP1** and **NP3** samples.

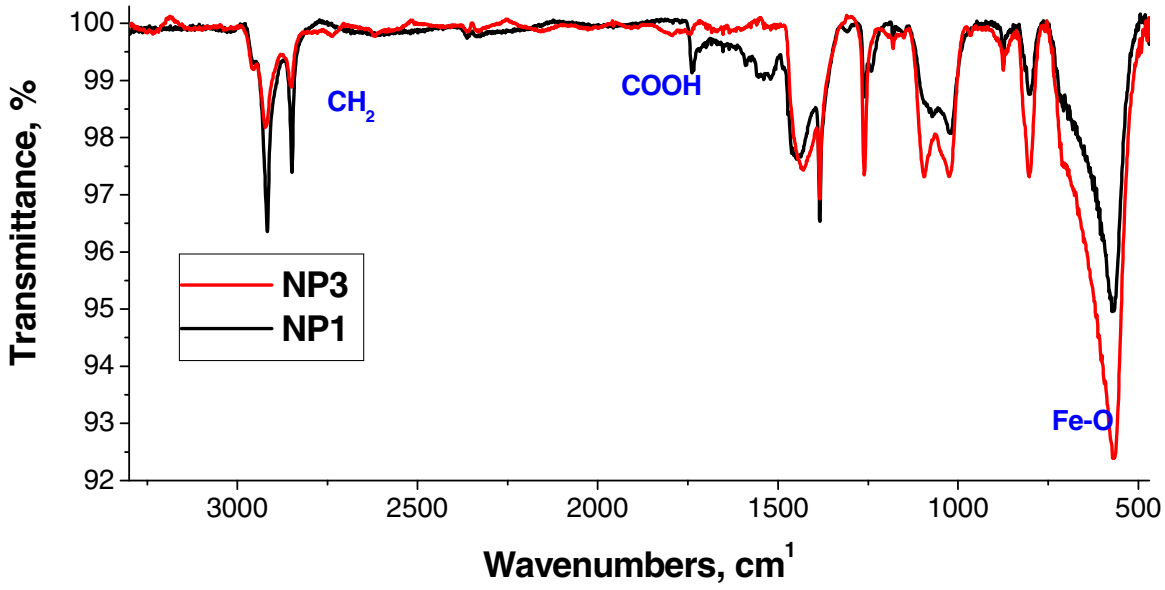

Figure S4. FTIR spectra of **NP1** and **NP3**.

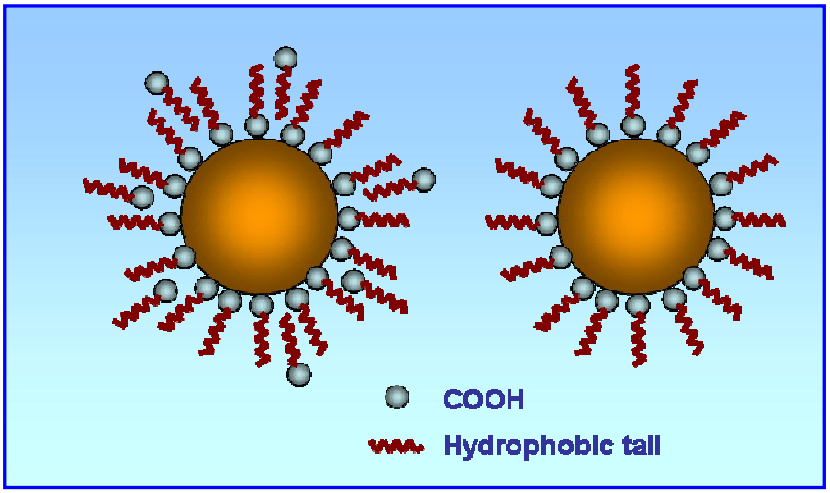

Scheme S1. Schematic representation of **NP1** (left) and **NP3** (right).

4. SAXS

In addition to modeling of the self-assembled PMAcOD particles in water using individual **-**MAcOD**-** molecules (as described in the main text) we also attempted to construct models from the building blocks consisting of ten **-**MAcOD**-** units obtained by molecular modeling (see Experimental part of the main text). The best models obtained were also disks with the diameter 40 nm and thickness 3.2 nm, similar to the modeling using individual **-**MAc-OD- units. The scattering patterns computed from the models built from short PMAcOD chains displayed peaks at higher angles due to their ridge-like structure (Figure S6, right panel). The accuracy of the scattering data was not sufficient to distinguish between the models from monomers or short chains but the shape of the self-assembled PMAcOD was clearly a disk-like bilayer.

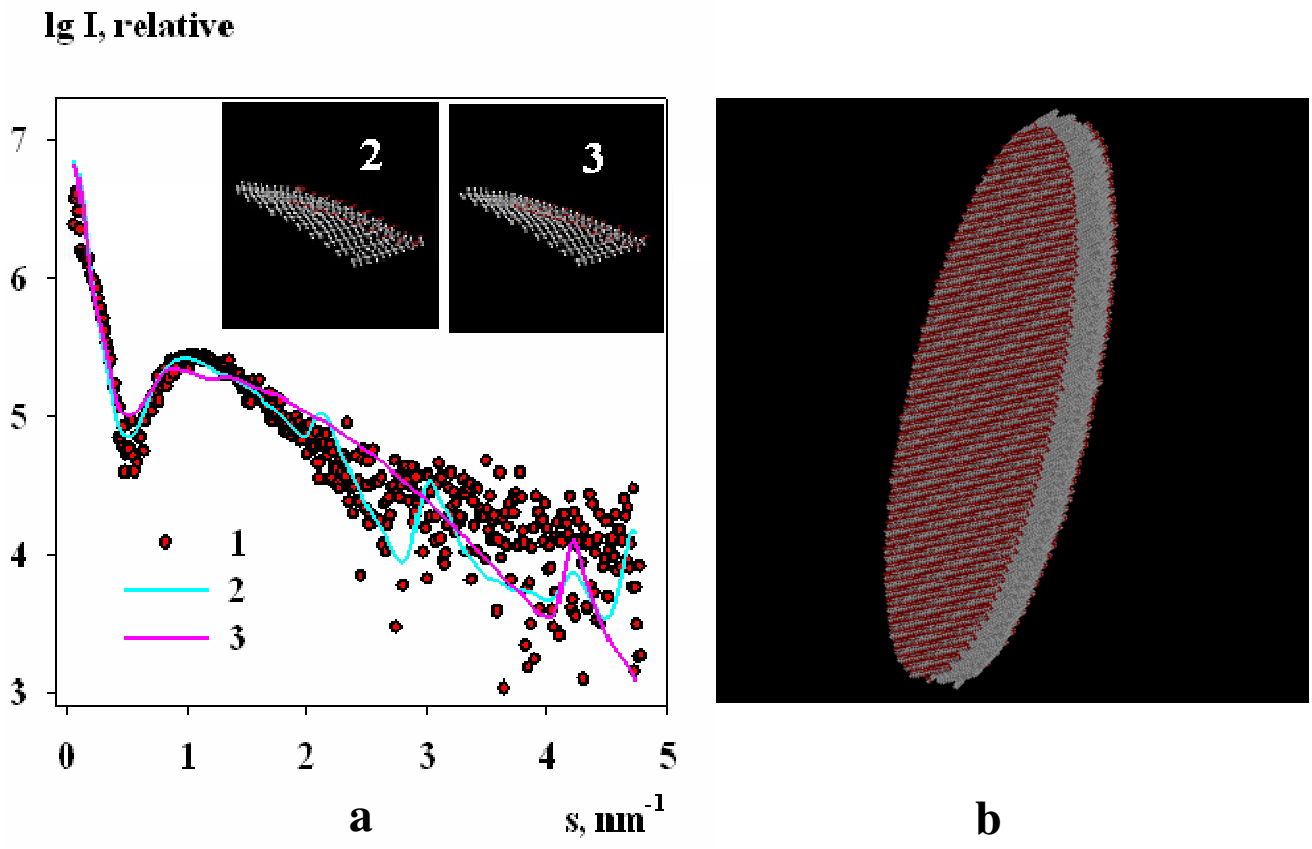

Figure S6. Left panel: the experimental data (1), scattering patterns computed for the disk-like models constructed from short PMAcOD polymer chains consisting of 10 RSS (2) and SSS (3) -MAc-OD- units. Right panel: the PDB-image of the disk-like model constructed from short **PMAcOD** polymer chains.

References

1. Bronstein, L. M.; Huang, X.; Retrum, J.; Schmucker, A.; Pink, M.; Stein, B. D.; Dragnea, B. *Chem. Mater.* **2007,** 19, (15), 3624.
2. Huang, X.; Bronstein, L. M.; Retrum, J. R.; Dufort, C.; Tsvetkova, I.; Aniagyei, S.; Stein, B.; Stucky, G.; McKenna, B.; Remmes, N.; Baxter, B.; Kao, C. C.; Dragnea, B. *Nano Lett.* **2007,** 7, (8), 2407.
3. Shtykova, E. V.; Huang, X.; Remmes, N.; Baxter, D.; Stein, B. D.; Dragnea, B.; Svergun, D. I.; Bronstein, L. M. *J. Phys. Chem. C ASAP* **2007**.
4. Lu, A.-H.; Salabas, E. L.; Schueth, F. *Angew. Chim. Int. Ed. and references therein* **2007,** 46, (8), 1222.
5. Drelich, J.; Jang, W.-H.; Miller, J. D. *Langmuir* **1997,** 13, (5), 1345.
6. Wang, L.; Bao, J.; Wang, L.; Zhang, F.; Li, Y. *Chemistry* **2006,** 12, (24), 6341.
7. Pal, B.; Sharon, M. *Thin Solid Films* **2000,** 379, (1,2), 83.